

# Spintronics of a Nanoelectromechanical Shuttle

D. Fedorets,\* L. Y. Gorelik, R. I. Shekhter, and M. Jonson  
*Department of Applied Physics, Chalmers University of Technology  
 and Göteborg University, SE-412 96 Göteborg, Sweden*  
 (Dated: December 2, 2024)

We study the effects of coupling between the spin degree of freedom of electrons and the shuttle phenomena in a nanoelectromechanical single-electron transistor with spin-polarized leads. It is shown that in such a system the shuttle effects can be controlled via external magnetic field. Different stable regimes of the spintronic NEM-SET operation are found and analyzed. Two types of transitions between stable states as a function of the magnetic and electric field are found.

Two branches of condensed matter physics — nanoelectromechanics [1, 2, 3] and spintronics [4] become more and more popular with the advances of modern technology. Both branches study the interplay between different degrees of freedom and ways to control one degree of freedom via its coupling to the others. Spintronics deals with the control and manipulation of the spin degree of freedom. Nanoelectromechanics studies the interplay between mechanical and electronic degrees of freedom. In particular, study of the coupling between elastomechanical degrees of freedom and electron tunneling has been attracting a lot of attention recently (see the review [5]).

In this paper we will study the effects of coupling between the spin degrees of freedom of electrons and elastomechanical degree of freedom. We will consider a simple model system — a nanoelectromechanical single-electron transistor (NEM-SET) with magnetic leads. A NEM-SET is a SET with a movable central island whose center-of-mass motion is confined by a harmonic potential. This simple system is very rich in nanoelectromechanical properties and was studied for the first time in [6] where an electromechanical instability was predicted — when one applies a high enough bias voltage between the leads the equilibrium position of the island becomes unstable and a new stable regime develops. In this regime the island oscillates with an amplitude determined by the balance between the energy pumped into the mechanical degree of freedom and dissipation. The stable regime oscillations alter drastically the electron transport properties of the system. After the publication of [6] different types of NEM-SET have been fabricated [7, 8, 9] and vibration mediated currents through them have been observed.

Recently, a lot of progress has been made in developing the quantum theory of shuttle phenomena in NEM-SETs [10, 11, 12, 13, 14, 15], but it was always assumed that the electron transport through the central island is not spin-polarized since no magnetic electrodes were involved. If the leads are magnetic and the electron transport is spin-polarized a new possibility opens up for "spintronical" control of the system, which allows us to manipulate the mechanical degrees of freedom by applying a magnetic field  $B$  between the leads. The magnetic field causes the spin of the electron on the island to precess with the frequency  $\omega_B \equiv g\mu_B B/\hbar$  ( $g$  is the electron  $g$  factor and  $\mu_B$  is the Bohr magneton). As a result, the coupled dynamics of the electronic and mechanical degrees of freedom can be controlled via the magnetic field. In this work we show that in the magnetic NEM-SET the instability threshold becomes dependent on the magnetic field. We will also determine the stable regimes of the spintronic NEM-SET operation under the experimentally relevant conditions.

The system under consideration is a NEM-SET with fully spin-polarized magnetic leads. All the electrons in the left lead are spin up and in the right lead — spin down. A symmetric bias voltage is applied, resulting in an electric field  $\mathcal{E}$  between the leads. We assume that the external magnetic field  $B$  is oriented perpendicular to the direction of the magnetization in the leads. The movable central island (dot) carries one single-electron energy level which is spin-degenerate in the absence of the magnetic field.

The following Hamiltonian is used to describe our system

$$H = \sum_{\alpha, k} \epsilon_{\alpha k} a_{\alpha k}^\dagger a_{\alpha k} + \sum_{\alpha, k} T_\alpha(X) [a_{\alpha k}^\dagger c_\alpha + c_\alpha^\dagger a_{\alpha k}] + [\epsilon_0 - e\mathcal{E}X] \sum_\alpha c_\alpha^\dagger c_\alpha - \frac{\hbar}{2} [c_\uparrow^\dagger c_\downarrow + c_\downarrow^\dagger c_\uparrow] + H_V + H_{V-B} + H_B. \quad (1)$$

Here the first term describes noninteracting electrons in leads ( $\alpha = L, R$ ) with constant densities of states  $\mathcal{D}$ . The operator  $a_{\alpha k}^\dagger$  ( $a_{\alpha k}$ ) creates (destroys) an electron with momentum  $k$  in the lead  $\alpha$  with the corresponding spin. The electrons in each lead are held at a constant electrochemical potential  $\mu_{L,R} = \mp eV/2$ , where  $e < 0$  is the electron charge and  $V > 0$  is the bias voltage. Since the leads are fully spin-polarized the lead index  $\alpha$  can also be used as a spin index:  $L = \uparrow$  and  $R = \downarrow$ . The second term represents tunneling of electrons (without spin flip) between the island and the leads. The operator  $c_\alpha^\dagger$  ( $c_\alpha$ ) creates (destroys) an electron with spin  $\alpha$  on the level in the dot. The

tunneling amplitudes depend exponentially on the displacement  $X$ :  $T_{L,R}(X) = T_0 \exp\{\mp X/\lambda\}$ . The third and fourth terms describe the single electronic state in the dot and its coupling to the magnetic field  $B$  and the electric field  $\mathcal{E}$ .  $h = g\mu_B B$  is the Zeeman splitting. The term

$$H_V \equiv \frac{P^2}{2M} + \frac{M\omega_0^2 X^2}{2} \quad (2)$$

describes the vibrational degree of freedom associated with the center-of-mass motion of the island. Here  $M$  is the mass of the island and  $\omega_0$  its vibration frequency. The last two terms represent the coupling  $H_{V-B}$  of the oscillator  $H_V$  to a heat bath  $H_B$ . We assume that this coupling is linear in  $X$  and treat it in the weak-coupling limit (see the discussion in [14] and references therein). For simplicity, we assume that the temperature is zero.

It is convenient to introduce dimensionless units and measure all lengths in units of the zero point oscillation amplitude  $x_0$ , all energies in units of  $\hbar\omega_0$  and time in units of  $\omega_0^{-1}$ . We also define dimensionless operators for the displacement,  $x \equiv X/x_0$ , and momentum,  $p \equiv x_0 P/\hbar$ .

After projecting out the leads and the thermal bath, one gets in the high bias voltage limit the following quantum master equation for the reduced density operator  $\rho(t)$  of the dot:

$$\dot{\rho} = -i [H_{dot}, \rho] + \mathcal{L}_T \rho + \mathcal{L}_\gamma \rho \quad (3)$$

where

$$H_{dot} \equiv [\epsilon_0 - xd] \sum_\alpha c_\alpha^\dagger c_\alpha - \frac{\hbar}{2} [c_\uparrow^\dagger c_\downarrow + c_\downarrow^\dagger c_\uparrow] + H_V, \quad (4)$$

$d \equiv e\mathcal{E}/(M\omega_0^2 x_0)$  is the shift in the equilibrium position of the oscillator caused by the electric field  $\mathcal{E}$  after an electron is placed in the dot,

$$\mathcal{L}_T \rho \equiv \pi \mathcal{D} \left[ 2T_L(x) c_\uparrow^\dagger \rho c_\uparrow T_L(x) - \{T_L^2(x) c_\uparrow c_\uparrow^\dagger, \rho\} + 2T_R(x) c_\downarrow^\dagger \rho c_\downarrow T_R(x) - \{T_R^2(x) c_\downarrow c_\downarrow^\dagger, \rho\} \right] \quad (5)$$

describes tunneling of electrons on and off the dot,

$$\mathcal{L}_\gamma \rho \equiv -\frac{i\gamma}{2} [x, \{p, \rho\}] - \frac{\gamma}{2} [x, [x, \rho]] \quad (6)$$

relates to the damping of vibrations,  $\{\bullet, \bullet\}$  denotes the anticommutator and  $\gamma \ll 1$  is the dissipation rate.

We will study analytically an experimentally relevant regime [7], where

$$\lambda \gg d \sim 1 \quad (7)$$

and  $\Gamma_0 \equiv 2\pi\mathcal{D}T_0^2 \ll 1$ .

The reduced density operator acts on the Hilbert space of the dot, which is the tensor product of the Hilbert space of the oscillator and the electronic space of the dot which is spanned by the four basis vectors:  $|0\rangle$ ,  $|\uparrow\rangle \equiv c_\uparrow^\dagger |0\rangle$ ,  $|\downarrow\rangle \equiv c_\downarrow^\dagger |0\rangle$  and  $|\downarrow\uparrow\rangle \equiv c_\downarrow^\dagger c_\uparrow^\dagger |0\rangle$ . The time evolution of the four diagonal elements  $\rho_0 \equiv \langle 0 | \rho | 0 \rangle$ ,  $\rho_\uparrow \equiv \langle \uparrow | \rho | \uparrow \rangle$ ,  $\rho_\downarrow \equiv \langle \downarrow | \rho | \downarrow \rangle$  and  $\rho_2 \equiv \langle \downarrow\uparrow | \rho | \downarrow\uparrow \rangle$  of the reduced density operator  $\rho$  in this basis is coupled to off-diagonal elements, but only to those that describe the correlations between the spin-up and spin-down states of the dot:  $\rho_{\uparrow\downarrow} \equiv \langle \uparrow | \rho | \downarrow \rangle$  and  $\rho_{\downarrow\uparrow} = \rho_{\uparrow\downarrow}^*$ .

After shifting the origin of the  $x$ -axis to the point  $x = d$ , the time evolution of the above diagonal elements and the off-diagonal elements  $\rho_{\uparrow\downarrow}$  and  $\rho_{\downarrow\uparrow}$  is determined by the following coupled system of equations of motion

$$\dot{\rho}_0 = -i [H_V + xd, \rho_0] - \frac{1}{2} \{ \hat{\Gamma}_L, \rho_0 \} + \sqrt{\hat{\Gamma}_R} \rho_\downarrow \sqrt{\hat{\Gamma}_R} + \mathcal{L}_\gamma \rho_0, \quad (8)$$

$$\dot{\rho}_\downarrow = -i [H_V, \rho_\downarrow] + i \frac{\hbar}{2} [\rho_{\uparrow\downarrow} - \rho_{\downarrow\uparrow}] - \frac{1}{2} \{ \hat{\Gamma}_+, \rho_\downarrow \} + \mathcal{L}_\gamma \rho_\downarrow, \quad (9)$$

$$\dot{\rho}_\uparrow = -i [H_V, \rho_\uparrow] - i \frac{\hbar}{2} [\rho_{\uparrow\downarrow} - \rho_{\downarrow\uparrow}] + \sqrt{\hat{\Gamma}_L} \rho_0 \sqrt{\hat{\Gamma}_L} + \sqrt{\hat{\Gamma}_R} \rho_2 \sqrt{\hat{\Gamma}_R} + \mathcal{L}_\gamma \rho_\uparrow, \quad (10)$$

$$\dot{\rho}_2 = -i[H_V - xd, \rho_2] - \frac{1}{2} \left\{ \hat{\Gamma}_R, \rho_2 \right\} + \sqrt{\hat{\Gamma}_L} \rho_\downarrow \sqrt{\hat{\Gamma}_L} + \mathcal{L}_\gamma \rho_2, \quad (11)$$

$$\dot{\rho}_{\uparrow\downarrow} = -i[H_V, \rho_{\uparrow\downarrow}] + i\frac{h}{2} [\rho_\downarrow - \rho_\uparrow] - \frac{1}{2} \rho_{\uparrow\downarrow} \hat{\Gamma}_+ + \mathcal{L}_\gamma \rho_{\uparrow\downarrow}, \quad (12)$$

$$\dot{\rho}_{\downarrow\uparrow} = -i[H_V, \rho_{\downarrow\uparrow}] - i\frac{h}{2} [\rho_\downarrow - \rho_\uparrow] - \frac{1}{2} \hat{\Gamma}_+ \rho_{\downarrow\uparrow} + \mathcal{L}_\gamma \rho_{\downarrow\uparrow}, \quad (13)$$

where  $\hat{\Gamma}_\alpha \equiv 2\pi\mathcal{D}T_\alpha^2(x+d)$  and  $\hat{\Gamma}_+ \equiv \hat{\Gamma}_L + \hat{\Gamma}_R$ .

One can find the stationary solution (steady state) of the above system perturbatively in the small parameters  $d/\lambda \sim \lambda^{-1}$  and  $\gamma$ . For this purpose it is convenient to work with a new set of density operators  $\rho_+ \equiv \rho_{0+2} + \rho_\downarrow + \rho_\uparrow$ ,  $\rho_{0\pm 2} \equiv \rho_0 \pm \rho_2$ ,  $\rho_{\downarrow-\uparrow} \equiv \rho_\downarrow - \rho_\uparrow$  and  $\rho_{\pm c} \equiv \rho_{\uparrow\downarrow} \pm \rho_{\downarrow\uparrow}$ .

We will use the Wigner function representation of the density operator  $\rho$ :

$$W_\rho(x, p) \equiv \frac{1}{2\pi} \int_{-\infty}^{+\infty} d\xi e^{-ip\xi} \left\langle x + \frac{\xi}{2} |\rho| x - \frac{\xi}{2} \right\rangle. \quad (14)$$

Rescaling the phase variables  $X \equiv x/\lambda$ ,  $P \equiv p/\lambda$  and changing to the polar coordinates  $X = A \sin \varphi$ ,  $P = A \cos \varphi$ , one obtains a steady-state equation for  $W_+$  that has the form

$$\partial_\varphi W_+ = \left\{ -\frac{\Gamma_+(X)}{2} \mathcal{C} + \mathcal{L}_\gamma \right\} W_+ + \left\{ \frac{d}{\lambda} \partial_P + \frac{\Gamma_-(X)}{2} \mathcal{C} \right\} W_{0-2} - \frac{\Gamma_+(X)}{2} \mathcal{C} W_{\downarrow-\uparrow}. \quad (15)$$

Here  $\Gamma_\pm(X) \equiv \Gamma_R(X) \pm \Gamma_L(X)$ ,  $\mathcal{L}_\gamma \equiv \gamma [\partial_P P + \frac{1}{2}\lambda^{-2}\partial_P^2]$  and  $\mathcal{C} \equiv \cosh [i\lambda^{-2}\partial_P] - 1$ .

Eq. (15) for the oscillator Wigner function,  $W_+$ , is coupled to the steady state equation for the vector-function  $\mathbf{W} \equiv [W_{0-2}, W_{\downarrow-\uparrow}, W_{-c}, W_{+c}, W_{0+2}]^T$ .

We will use second order perturbation theory in the small parameters  $d/\lambda$  and  $\gamma$ , which was developed in Ref. [12]. To apply this theory, one has to expand Eq. (15) to second order in  $d/\lambda$  and  $\gamma$ ,

$$[\partial_\varphi - \gamma \partial_P P] W_+ = \frac{d}{\lambda} \partial_P W_{0-2}, \quad (16)$$

and the steady state equations for the vector-function  $\mathbf{W}$  to the first order,

$$\partial_\varphi W_{0-2} = \left\{ -\frac{\Gamma_+(X)}{2} + \gamma \partial_P P \right\} W_{0-2} + \frac{d}{\lambda} \partial_P W_{0+2} + \frac{\Gamma_-(X)}{2} W_{\downarrow-\uparrow} + \frac{\Gamma_-(X)}{2} W_+, \quad (17)$$

$$\partial_\varphi W_{\downarrow-\uparrow} = \left\{ -\frac{\Gamma_+(X)}{2} + \gamma \partial_P P \right\} W_{\downarrow-\uparrow} - h W_{-c} + \frac{\Gamma_-(X)}{2} W_{0-2} - \frac{\Gamma_+(X)}{2} W_+, \quad (18)$$

$$\partial_\varphi W_{-c} = \left\{ -\frac{\Gamma_+(X)}{2} + \gamma \partial_P P \right\} W_{-c} + h W_{\downarrow-\uparrow}, \quad (19)$$

$$\partial_\varphi W_{0+2} = \{-\Gamma_+(X) + \gamma \partial_P P\} W_{0+2} + \frac{\Gamma_+(X)}{2} W_{\downarrow-\uparrow} + \left\{ \frac{d}{\lambda} \partial_P + \frac{\Gamma_-(X)}{2} \right\} W_{0-2} + \frac{\Gamma_+(X)}{2} W_+. \quad (20)$$

The equation for  $W_c$  is omitted, because it decouples from the rest.

Using the projector formalism developed in Ref. [12], we obtain that in the leading order approximation the oscillator Wigner function  $W_+(A, \varphi)$  is  $\varphi$ -independent and is determined by

$$\partial_A A [f(A) + D(A) \partial_A] W_+(A) = 0, \quad (21)$$

where

$$f(A) \approx \frac{A}{2} \left[ \gamma - \frac{d}{\lambda} \beta_0(A) \right], \quad \beta_0(A) \equiv -\frac{1}{\pi A} \int_0^{2\pi} d\varphi \cos \varphi G_{0-2}^{(0)}(\varphi) \geq 0, \quad (22)$$

$\mathcal{Z}$  is a normalization constant and  $D(A) > 0$  is of the second order in  $d/\lambda$  and  $\gamma$ . The function  $G_{0-2}^{(0)}(\varphi)$  is determined by the system of differential equations:

$$\partial_\varphi G_{0-2}^{(0)} = -\frac{\Gamma_+(X)}{2} G_{0-2}^{(0)} + \frac{\Gamma_-(X)}{2} G_{\downarrow-\uparrow}^{(0)} + \frac{\Gamma_-(X)}{2}, \quad (23)$$

$$\partial_\varphi G_{\downarrow-\uparrow}^{(0)} = \frac{\Gamma_-(X)}{2} G_{0-2}^{(0)} - \frac{\Gamma_+(X)}{2} G_{\downarrow-\uparrow}^{(0)} - h G_{-c}^{(0)} - \frac{\Gamma_+(X)}{2}, \quad (24)$$

$$\partial_\varphi G_{-c}^{(0)} = h G_{\downarrow-\uparrow}^{(0)} - \frac{\Gamma_+(X)}{2} G_{-c}^{(0)}, \quad (25)$$

with  $2\pi$ -periodic boundary conditions.

It follows from Eq. (21) that the oscillator Wigner function  $W_+$  has the form

$$W_+(A) \approx \mathcal{Z}^{-1} \exp \left\{ - \int_0^A dA \frac{f(A)}{D(A)} \right\}, \quad (26)$$

and is peaked at points  $A_M$  determined by the conditions  $A_M [\gamma\lambda/d - \beta_0(A_M)] = 0$  and  $f'(A_M) > 0$ . In the vicinity of these points,  $W_+(A)$  can be approximated by a narrow Gaussian with the variance  $\sigma^2 \equiv D(A_M)/f'(A_M)$ .

Solving the system of Eqs. (23,24,25) in the vicinity of  $A = 0$ , we obtain

$$\beta_0(A) = \Gamma_0 \frac{2h^2}{h^2 + \Gamma_0^2} + \mathcal{O}(A^2), \quad A \rightarrow 0. \quad (27)$$

The positive function  $\beta_0(A, h)$  is bounded, has only one maximum and monotonically decreases for large  $A$  (Fig. 1). One can show that if  $h < \Gamma_0\sqrt{3}$ , the function  $\beta_0(A)$  has its only maximum at  $A = 0$ , while if  $h > \Gamma_0\sqrt{3}$ , the function  $\beta_0(A)$  has a minimum there.

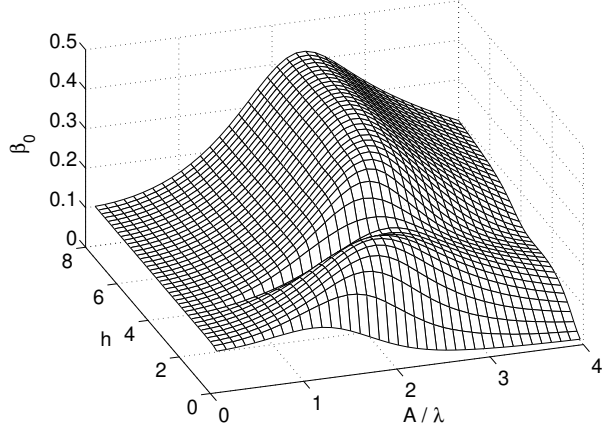


FIG. 1: The function  $\beta_0(A, h)$  (for  $\Gamma_0 = 0.05$ ).

The above structure of the function  $\beta_0(A, h)$  determines the steady state regimes of the magnetic NEM-SET operation in the two-dimensional parametric space  $d - h$ , which is summarized in Fig. 2 in the form of a "phase diagram".

If  $d/(\gamma\lambda) < 1/[\max \beta_0(A)](h)$ , the only stable point is  $A = 0$  ("the ground state phase"). If  $1/[\max \beta_0(A)](h) < d/(\gamma\lambda) < (h^2 + \Gamma_0^2)/(2h^2\Gamma_0)$ , there are two stable points:  $A = 0$  and  $A = A_C$  ("the bistable phase"). And if  $d/(\gamma\lambda) > (h^2 + \Gamma_0^2)/(2h^2\Gamma_0)$ , there is only one stable point:  $A = A_C \neq 0$  ("the shuttle phase").

One can show that there are two types of "phase" transitions in our system: the continuous phase transition and the first-order phase transition. The former occurs when one crosses the border between the ground state phase and the shuttle phase. In this case the stable amplitude  $A$  changes continuously as a function of the electric (Fig. 3)

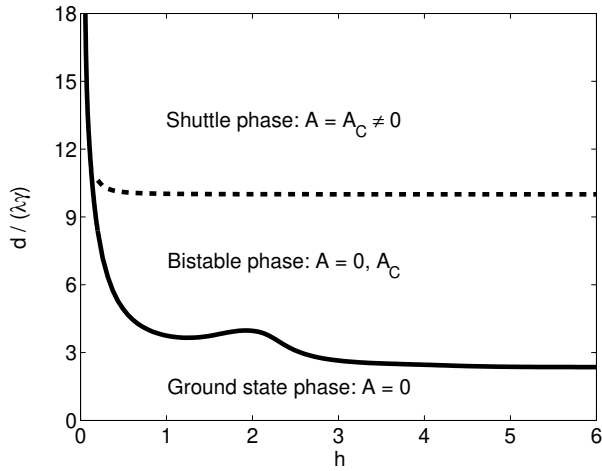


FIG. 2: "Phase diagram" in the  $d - h$  plane (for  $\Gamma_0 = 0.05$ ).

and magnetic field. The latter happens when one moves from the ground state phase to the shuttle phase through the bistable phase. Then the steady state amplitude changes in a jump-like fashion (Fig. 4). The first-order phase transition depends on the direction in which one moves between the phases. As a result one has a hysteretic effect (Fig. 4).

The steady state current through the system is given by

$$I = e \text{Tr} \left\{ \hat{\Gamma}_L(x) (\rho_0 + \rho_\downarrow) \right\} \equiv \frac{e}{2} \int dX dP \Gamma_L(X) [W_+ + W_{0-2} + W_{\downarrow-\uparrow}], \quad (28)$$

which in the lowest order in  $d/\lambda$  and  $\gamma$  reads

$$I \approx \frac{e}{4\pi} \left\langle \int_0^{2\pi} d\varphi \Gamma_L(X) [1 + G_{0-2}^{(0)} + G_{\downarrow-\uparrow}^{(0)}] \right\rangle \equiv \langle I_{cl}(A) \rangle, \quad (29)$$

where  $\langle \bullet \rangle \equiv 2\pi \int_0^\infty dA A W_+(A) [\bullet]$  and  $G_{0-2}^{(0)}$  and  $G_{\downarrow-\uparrow}^{(0)}$  are determined by the system of Eqs. (23,24,25).

The current in the continuous and first order transition regimes is shown in Figs. 5 and 6

In conclusion, we have considered shuttle phenomena in a NEM-SET with spin-polarized leads. We have shown, that coupling between the spin-polarized electronic transport and the center-of-mass motion of the island allows us to control the dynamics of the mechanical degree of freedom via the external magnetic field. The different stable regimes of the magnetic NEM-SET operation were found and transitions between them caused by the variations of the electric and magnetic fields were analyzed.

Financial support from the Swedish Foundation for Strategic Research (DF, LYG, RIS) and the Swedish Research Council (LYG,RIS) is gratefully acknowledged.

---

\* dima@fy.chalmers.se

- [1] M. L. Roukes, Physics World **14**, 25 (2001).
- [2] A. N. Cleland, Foundations of Nanomechanics (Springer) 2003.
- [3] M. Blencowe, Phys. Rep. **395**, 159 (2004).
- [4] I. Zutic, J. Fabian, and S. Das Sarma, Rev. Mod. Phys. **75**, 715 (2004).
- [5] R. I. Shekhter *et al.*, J. Phys. C **15**, R441 (2003).
- [6] L. Y. Gorelik *et al.*, Phys. Rev. Lett. **80**, 4526 (1998); A. Isacsson *et al.*, Physica B **255**, 150 (1998).
- [7] H. Park *et al.*, Nature **407**, 57 (2000).
- [8] A. Erbe, C. Weiss, W. Zwerger, and R.H. Blick, Phys. Rev. Lett. **87**, 0961061 (2001).
- [9] D.V. Scheible, and R.H. Blick, Appl. Phys. Lett. **84**, 4362 (2004).
- [10] D. Fedorets *et al.*, Europhys. Lett. **58**, 99 (2002).
- [11] D. Fedorets, Phys. Rev. B **68**, 033106 (2003).

- [12] D. Fedorets *et al.*, Phys. Rev. Lett. **92**, 166801 (2004).
- [13] A. D. Armour and A. MacKinnon, Phys. Rev. B **66**, 035333 (2002).
- [14] T. Novotny, A. Donarini, and A.-P. Jauho, Phys. Rev. Lett. **90**, 256801 (2003).
- [15] A. Y. Smirnov, L. G. Mourokh, and N. J. M. Horing, Phys. Rev. B **69**, 115310 (2004).

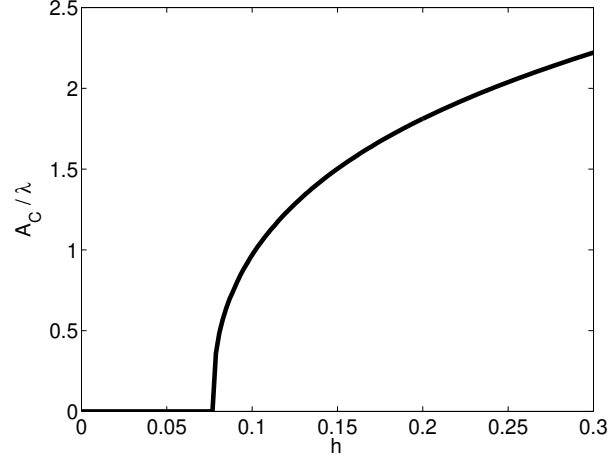


FIG. 3: The steady-state amplitude  $A_C$  in the continuous transition regime (for  $\Gamma_0 = 0.05$  and  $d/(\gamma\lambda) = 14.3$ ).

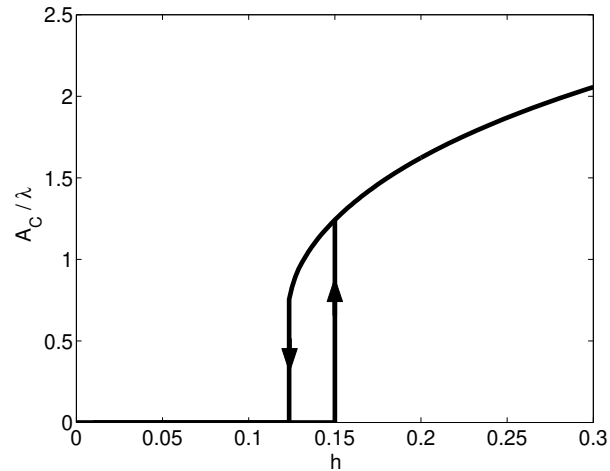


FIG. 4: Hysteretic behavior of the steady state amplitude  $A_C$  in the first-order transition regime (for  $\Gamma_0 = 0.05$  and  $d/(\gamma\lambda) = 11.1$ ).

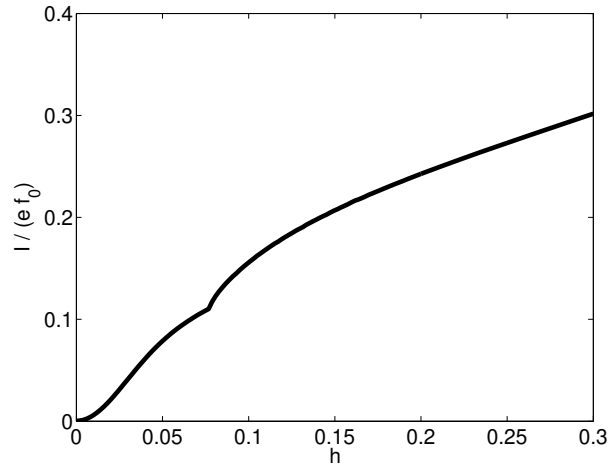


FIG. 5: The steady-state current in the continuous transition regime (for  $\Gamma_0 = 0.05$  and  $d/(\gamma\lambda) = 14.3$ ).

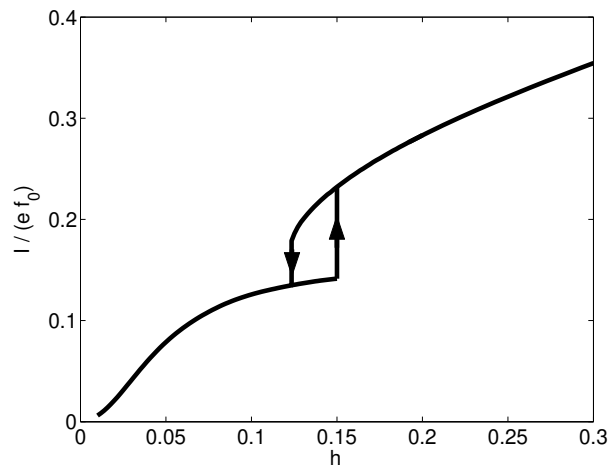


FIG. 6: Hysteretic behavior of the steady state current in the first-order transition regime (for  $\Gamma_0 = 0.05$  and  $d/(\gamma\lambda) = 11.1$ ).